



Probabilistic Harmonic Estimation in Uncertain Transmission Networks Using Sequential ANNs

DOI:

[10.1109/ICHQP53011.2022.9808840](https://doi.org/10.1109/ICHQP53011.2022.9808840)

Document Version

Final published version

[Link to publication record in Manchester Research Explorer](#)

Citation for published version (APA):

Zhao, Y., & Milanovic, J. V. (2022). Probabilistic Harmonic Estimation in Uncertain Transmission Networks Using Sequential ANNs. In *2022 20th International Conference on Harmonics & Quality of Power (ICHQP)* (pp. 1-6) <https://doi.org/10.1109/ICHQP53011.2022.9808840>

Published in:

2022 20th International Conference on Harmonics & Quality of Power (ICHQP)

Citing this paper

Please note that where the full-text provided on Manchester Research Explorer is the Author Accepted Manuscript or Proof version this may differ from the final Published version. If citing, it is advised that you check and use the publisher's definitive version.

General rights

Copyright and moral rights for the publications made accessible in the Research Explorer are retained by the authors and/or other copyright owners and it is a condition of accessing publications that users recognise and abide by the legal requirements associated with these rights.

Takedown policy

If you believe that this document breaches copyright please refer to the University of Manchester's Takedown Procedures [<http://man.ac.uk/04Y6Bo>] or contact uml.scholarlycommunications@manchester.ac.uk providing relevant details, so we can investigate your claim.



Probabilistic Harmonic Estimation in Uncertain Transmission Networks Using Sequential ANNs

Yuqi Zhao
the University of Manchester
 Manchester, UK
 yuqi.zhao@postgrad.manchester.ac.uk

Jovica V. Milanović
the University of Manchester
 Manchester, UK
 jovica.milanovic@manchester.ac.uk

Abstract—In the face of transition towards the decarbonisation, increasing penetration level of power electronic interfaced renewable connections such as wind farms and PV plants are constantly influencing the uncertainties of transmission network and leading to additional uncontrolled harmonic power flows. These potential harmonic distortion issues could result in significant financial losses. To address this problem, the estimation of harmonic propagation through transmission network with increasing penetration of nonlinear loads, power electronics based renewable generation and control devices is becoming increasingly important. This paper proposes a comprehensive framework of applying sequential artificial neural network (ANN) techniques to estimate individual order harmonic distortions and total harmonic distortions (THD) at unmonitored buses in large uncertain transmission networks based on offline measurements and simulations. This study will contribute to facilitate the standard compliance, reduce the extent of the monitor installation, accelerate the assessment of harmonic performance and mitigation studies, as well as contribute to the forecast of potential harmonic issues in large transmission system.

Index Terms--ANN, harmonic estimation, power electronics, renewable energy source, transmission system

I. INTRODUCTION

Decarbonisation requires increasing penetration level and reliance on low carbon generation, storage and demand technologies, majority of which is connected to the network through power electronic (PE) interface. Additionally flexible alternating current transmission system (FACTS) devices and high voltage direct current (HVDC) transmission lines are increasingly used to improve efficiency, flexibility and security of electricity supply. Such trend might result in increasing challenges posed by the power quality problems. Among those, the harmonic distortion issues, that result in significant financial losses to both network operators and end users is becoming even more pronounced. Although the harmonic distortions and voltage fluctuation are controlled by transmission system operators (TSOs) at present, the increased number of the future PE devices could lead to increase propagation of harmonics into the transmission system and leading to additional uncontrolled harmonic power flows [1, 2].

Prediction of harmonic propagations is one of the main solutions to effectively anticipate and mitigate the power quality problems. The power system is highly dynamic in nature, which requires the supervising of harmonic distortions to be also adaptive. However, in reality, it is impossible to install harmonic analyzers/harmonic meters/power quality monitoring devices at every bus in the large transmission system due to the financial and technical reasons [3]. Therefore, it is necessary for TSOs to be able to estimate and

evaluate the harmonic performance of unmonitored buses based on the available harmonic measurements at monitored buses, so as to control the harmonic performance in the whole system.

One traditional solution to this problem is the harmonic state estimation (HSE) method, which utilizes the harmonic measurements at monitored buses and the network model to estimate the harmonic distortion level of other non-monitored locations [3-5]. Research such as [6] proposed several optimal monitor-placement methods for HSE. In the meantime, with the rapid improvement of computer science technologies and various computational algorithms, the ANN-based techniques [7] have become frequently and widely combined with HSE method to estimate power system harmonics. For example, for improving noise tolerance level [8], for improving the estimation precision and accelerating convergence [9-11], for faster and more accurate power system harmonic detection [12-14], for harmonic coefficients and relative phase shifts detection [15], for on-line tracking of harmonics [16, 17], for distinguishing between load contributed harmonics and supply harmonics [18, 19], etc.

Nevertheless, the application of HSE in transmission system is still very challenging since it requires a large number of synchronized monitoring devices to make the system fully observable [3-5]. Also, the measurement functions of HSE is related to the specific topology of the system and the configuration of measurement points, which are usually unknown in real-world scenarios because it is difficult to track the real-time operational structure of the network. These fundamental shortcomings render it of limited practical value.

This paper proposes a comprehensive assessment framework based on application of sequential ANNs to estimate individual order harmonic distortions and THD at unmonitored buses in large uncertain transmission networks using the offline measurements and Monte Carlo (MC) simulations. In Section II, the database of harmonic measurements is generated by large number of MC simulations in a modified IEEE 68-bus NETS-NYPS test network. Different probabilistic distributions and data ranges are adopted to model different operating conditions and uncertainties caused by emerging power system connections such as wind farms, PV plants, load demands and their corresponding unbalanced harmonic injections. Section III provides the detailed architecture of the proposed ANN model and the entire THD estimation methodology. A two-layer feed-forward ANN model with different hidden layer sizes and training algorithms is trained so that an appropriate ANN architecture can be adopted to accurately estimate the harmonic distortions in transmission network. Case studies regarding the development of the proposed ANN structure, start with the estimation of individual harmonics and finish

with the estimation of THD at every unmonitored bus in the network. They have been described and discussed in Section IV. Finally, the proposed THD estimation methodology has been validated against the harmonic measurements from different operating weeks.

II. POWER SYSTEM MODELLING

A. Test Network

In order to obtain the database of harmonic measurements suitable for ANN training, a modified IEEE 68-bus New England Test System-New York Power System (NETS-NYPS) test network (shown in Fig. 1) was simulated using Monte Carlo based probabilistic approach considering various system operation conditions caused by uncertainties [20, 21]. It is a 230 kV transmission system which consists of 68 buses in five geographical areas. Apart from the original 16 synchronous generators (G1-G16), the model is modified to integrate 20 renewable energy generations, i.e., 10 wind farms and 10 PV plants. The wind turbines are modelled as either Type 3 doubly fed induction generators (DFIG) or Type 4 Full Converter Connected (FCC) interfaced generator, while the PV panels are fully modelled as the FCC type of generators. In this research, the penetration level of RES is set as 60%. There are a total of 35 loads in the system, the industrial type and distribution network (DN) type of loads. They are modelled as a combination of linear and non-linear components. The percentage of nonlinear components of industrial loads and DN loads are assumed to be 50% and 20%, respectively.

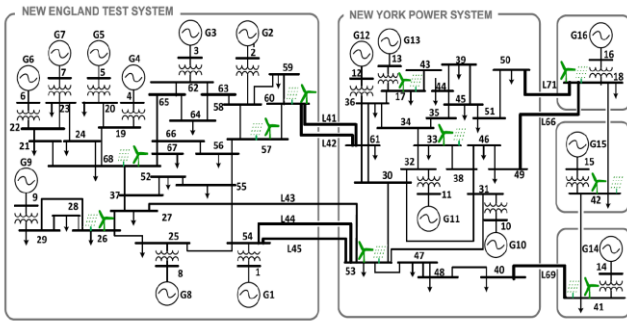


Fig. 1. Modified IEEE 68-bus NETS-NYPS test network.

The test network was modelled and simulated in the DigSILENT/PowerFactory environment [22, 23], where harmonic load flow was performed.

B. Modelling of Uncertainties

To address the uncertainties of this network, operating conditions with varying loading, PV and wind output are obtained from actual renewable generation profiles in one week in Europe in 2016 [24]. The probabilistic scaling factors utilised to represent the operating uncertainties of RES and load demand are updated every 10-min interval, in accordance with the time step required by standard IEEE519 [25]. The probabilistic output/loading scaling factors of wind, PV plants and loads are assumed to be sampled by following Weibull distribution ($\varphi=11.1, k=2.2$), Beta distribution ($\alpha=13.7, \beta=1.3$) and Normal distribution ($\mu=1, \sigma=0.033$), respectively [21].

C. Modelling of Harmonic Injections

As the major harmonic sources in transmission network, the PE interfaced wind farms, PV plants and non-linear load demands are modelled as harmonic current sources with 3-phase unbalanced magnitudes and phase angle injections over

multiple time intervals. For each type of harmonic sources, different harmonic injection spectra are utilised, covering different operating conditions. The magnitudes of harmonic injections are randomly sampled within normal distributed pre-defined ranges that are selected based on long-term measurements of the harmonic spectrum of PE interfaced generations [1, 20, 26]. For all types of harmonic sources, the harmonic angle injections are randomly sampled within a range of ($0^\circ, 180^\circ$), considering all 2nd-25th harmonic orders [26]. From the perspective of entire test network, harmonics injected from individual wind farm, PV plant and non-linear loads are obtained by multiplying the appropriate coefficient of harmonic spectrum sampled from the predefined harmonic ranges by their corresponding fundamental current. In order to include the uncertainties of harmonic injections, the probabilistic harmonic propagation simulation approach is conducted based on the Monte Carlo simulation technique where each harmonic current injection (magnitude and angle) of individual harmonic sources, for each of the three phases, are varied randomly by sampling uniform distributions (considering 10 or 20 random samples per period) within the given ranges.

III. METHODOLOGY

A two-layer feed-forward ANN, similar to the structure introduced in [27-29], is adopted to estimate the harmonic distortion in transmission network in this study. It is chosen as it is the most commonly used architecture that can potentially represent the non-linear relationship between the input and target as long as an appropriate hidden layer size is assigned.

A. Selection of Hidden Layer Size and Training Algorithm

The transfer functions of the hidden and output layer are log-sigmoid and tan-sigmoid, respectively, as suggested in [27-29]. Research [7] shows that the number of hidden layer neurons is not only related to the number of neurons in the input and output layer, but also related to the factors such as the complexity of the problem to be solved, the type of the transfer function, and the characteristics of the sample data. Therefore, a practical case study combining all these factors is carried out to determine an appropriate hidden layer size based on different calculation equations (listed in Table I) reported in published papers [30-31]. As a preliminary study, this case only considers one-day, single-phase, single-order (5th) harmonic measurements. Results of the training time and mean square errors (MSEs) are summarised in Table I. The ANN architecture was established and modified in MATLAB. All the trainings were performed with a processor of Intel® Core™ i7-4770 CPU @ 3.4GHz.

Taking the realistic circumstances into consideration, it is assumed that the monitored buses (52 buses in total) are the buses with connected synchronous generation or RES (26 in total) and 35 load buses (including both industrial and DN types of loads). It should be note that at some buses there are both generators, conventional and renewable, and loads connected. Therefore, in this case, the harmonic measurements (obtained by simulating the NETS-NYPS test network) from these 52 monitored buses and the other 16 unmonitored buses are set as the inputs and the targets of ANN, respectively. Regarding the equations list in Table I, the variables n , N_i and N_o stand for the number of neurons in hidden layer, input layer ($N_i=58$) and output layer ($N_o=16$), respectively. Parameters N_t represents the number of training pairs, which equals to 1440 ($24*6*10=1440$) in this case.

In order to compare different ANN training algorithms, both Levenberg-Marquardt Backpropagation (LMBP) and Bayesian Regularization Backpropagation (BRBP) are adopted. The LMBP training algorithm generally has the fastest convergence for networks with hundreds of weights. This advantage is particularly evident when very accurate training is required. The BRBP training algorithm usually takes longer but may be better for challenging problems [7].

TABLE I. RESULTS OF ANN TRAINING TIME AND MSE CONSIDERING DIFFERENT HIDDEN LAYER SIZES AND TRAINING FUNCTIONS

Ref.	Calculated hidden layer sizes	Training function	MSE (10^{-5})	Training time
[30]	$n = \frac{4Ni^2 + 3}{Ni^2 - 8} \approx 4$	trainlm trainbr	14.43 15.07	38 s 6 s
[32]	$n = \frac{\sqrt{1 + 8Ni} - 1}{2} \approx 10$	trainlm trainbr	3.808 3.253	24 s 1 min
[33]	$n = c \sqrt{\frac{Nt}{Ni + \ln Nt}}$, $Nt/Ni > 30$ $n = Nt/Ni \approx 28$, $Nt/Ni \leq 30$	trainlm trainbr	0.916 0.475	2-10 min 33 min
[34]	$n = \sqrt{Ni * No} \approx 29$	trainlm trainbr	0.970 0.460	5-10 min 42 min
[35]	$n = \log_2(Ni + 1) - No \rightarrow$ null	-	-	-
[36]	$n = 2^{Ni}/Ni + 1 \rightarrow$ too large	-	-	-
[35]	$n = 2^{Ni} - 1 \rightarrow$ too large	-	-	-

It can be seen from Table I that in order to both avoid the overfitting problem/large MSEs during training and ensure sufficiently good network performance, in other words, to take as few hidden layer neurons as possible under the condition that the error is within an acceptable range, a hidden layer with 28 neurons is chosen to be used in the following studies. It was also found that compared with using the BRBP (noted by *trainbr*) as training function, using the LMBP (noted by *trainlm*) training function can speed up the training time by several minutes. Therefore, the training function of ANN training is set as *trainlm* in the following studies.

B. Adopted ANN Structure

In this study, two different neural networks, namely ANN1 and ANN2 are adopted continuously to estimate THD values at unmonitored buses in the system. ANN1 is a two-layer feed-forward neural network with 52 input-layer neurons (represent for 52 monitored buses), 28 hidden-layer neurons and 16 output-layer neurons (represent for 16 unmonitored buses). ANN2 is also a two-layer feed-forward neural network, but with 24 input-layer neurons (represent for 24 individual harmonic orders), 28 hidden-layer neurons and single output-layer neuron (represent for THD at an unmonitored bus). Both ANN models are trained by LMBP training function. The transfer functions of the hidden and output layer are log-sigmoid and tan-sigmoid, respectively. The block diagram of entire THD estimation methodology is shown in Fig. 2.

In ANN1, the harmonic measurements of each individual harmonic (from 2nd to 25th) at monitored buses from previous week are set as the input. From the same week, the corresponding individual order of harmonic distortions at the unmonitored buses are set as the target. After training this ANN1, there will be 24 independent black boxes (representing

different specific harmonic orders) mapping the relationship between the harmonic distortions at monitored buses and unmonitored buses. Then, from the target week, the measured individual harmonic distortions at monitored buses can be fed into their corresponding black box as the input. By doing this, the required estimated harmonic distortions at unmonitored buses for the target week can be obtained as the outputs of individual black boxes. Different orders of harmonic distortions are trained separately by using a *for* loop.

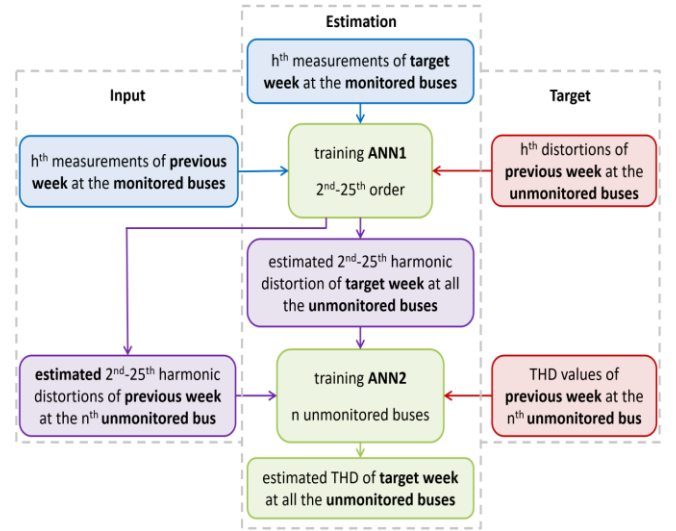


Fig. 2. Block diagram of THD estimation methodology.

In ANN2, from the perspective of individual buses, different orders of harmonic distortions at the same unmonitored bus from the previous week are reorganised and combined together and are considered as the input of ANN2. The target of ANN2 is set as the THD values on the corresponding unmonitored bus. After training this ANN2, there are n (number of unmonitored buses) independent black boxes mapping the relationship between all 2nd-25th harmonic orders and THD on this specific bus. Then, for the target week, the reorganised harmonic distortions of individual unmonitored buses, estimated by ANN1, can be fed into their corresponding black box as the input. Thereby, the required estimated THD of each unmonitored bus of the target week can be obtained as the output of individual black boxes. Different unmonitored buses are trained separately by using a *for* loop.

The main purpose of connecting two continuous ANN architectures is to compress the 3-dimensional relevant parameters, i.e., different orders of harmonic distortions, different unmonitored/monitored buses and different number of training samples into 2-dimensional inputs which are suitable for the training of two ANN architectures. During the testing stage of the algorithm, it was found that it is inaccurate to simply calculate the estimated THD in voltage (THD_v) using the equation (1). This is because generally the actual THD values in a power system include more than a few orders of harmonic distortions as well as inter-harmonic distortions. This is also the reason why ANN2 is applied in this study. Detailed discussions can be found in section IV. B.

$$THD_v(\%) = \frac{\sqrt{\sum_{h=2}^{\infty} V_h^2}}{V_1} \quad (1)$$

In this study, the absolute error (AE), defined by (2) and the relative error (RE), defined by (3) are utilised to evaluate

the estimation accuracy of the proposed ANN architecture. t_i and a_i stand for the estimated value and the actual value of a sample i , respectively.

$$\text{absolute error} = t_i - a_i \quad (2)$$

$$\text{relative error} = \frac{t_i - a_i}{a_i} * 100\% \quad (3)$$

IV. CASE STUDY

A. Estimation of Individual Harmonics

As a preliminary study, 5th, 7th, 11th, 13th harmonics are trained individually in this case. Taking the 5th harmonic as an example, Fig. 3 combines the fitted probability density functions (PDFs) of the absolute estimation errors at different unmonitored buses. As expected, this ANN architecture can satisfy the requirement of limiting the mean square error below a predetermined value, which is 10^{-5} in this case. The expected training time for individual harmonic order is less than 10 min.

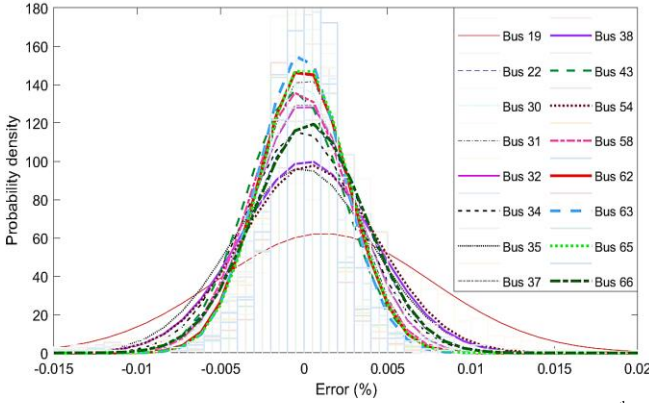


Fig. 3. Fitted PDFs of absolute error between actual and estimated 5th harmonic distortion at all unmonitored buses.

It can be seen that the mean values of the fitted errors at different buses are all concentrated at 0%, with the span of $\mu \pm 3\sigma$ within a narrow range of $\pm 0.005\%$. It should be noted that the ' $\pm 0.005\%$ ' indicates that if the actual value of 5th harmonic distortion is 0.2%, the estimated 5th harmonic distortion will be located within a range of (0.195%-0.205%). Among all the unmonitored buses, Bus 19 is the most critical one since the error distribution of this bus has larger mean value and wider spread. Therefore, in order to compare the results of multi-order harmonics, Bus 19 is selected as the target bus.

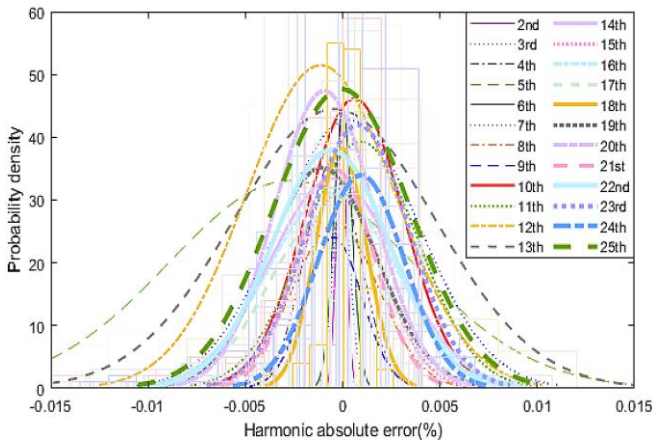


Fig. 4. Fitted PDFs of absolute error of 95th percentile 2nd-25th harmonics at Bus 19.

In order to avoid the extreme circumstances caused by the uncertainties, it is a common practice to take the 95th percentile value of harmonics as a comparison [25]. Therefore, Fig. 4 shows the fitted PDFs of absolute estimation error of 95th percentile for 2nd-25th harmonic at Bus 19. The variation of 5th estimated and actual harmonic distortions during the day is shown in Fig. 5.

It can be seen that the mean values of all fitted error curves are approximately concentrated at 0% and the errors are distributed within a narrow spread of $\pm 0.01\%$. For a single 5th harmonic order, the variations of the estimated harmonic distortions during the day at Bus 19 are roughly following the same trend of their actual values. This proves that the proposed ANN1 structure is able to accurately predict various orders of harmonic distortions at unmonitored buses.

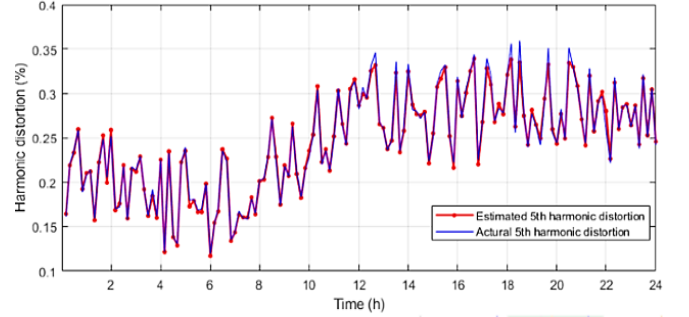


Fig. 5. Comparison of estimated and actual 5th harmonic on Bus 19.

B. Estimation of THD

As mentioned in section III. B, this study compares two approaches of estimating THD at unmonitored bus.

The first approach is to calculate THD using the equation (1), based on limited number of individual harmonics estimated by ANN1, relying on corresponding harmonic measurements at the monitored buses.

The second method is to estimate THD with the help of artificial intelligence, i.e. using the proposed architecture of ANN2 (detailed in section III. B), also based on limited number of monitored harmonic orders.

According to standard EN 50160 [37], typical upper limit for harmonic measurements in Europe transmission system is 50th harmonic, however if the risk of resonance at higher harmonics is low, the upper limit can also be the 25th harmonic. Therefore, only 2nd-25th harmonic are considered in this study. According to the fitted PDFs of absolute prediction errors of 95th percentile THD at all unmonitored buses, Table II summarises the ranges of mean values and distributions of the fitted absolute errors when using different THD estimation methods. It can be seen that after training ANN2, the distribution range of THD absolute errors has been reduced by approximately 94% $((0.5-0.03)/0.5=0.94\%)$, which perfectly enhances the accuracy.

TABLE II. COMPARISON OF THE RANGE OF MEAN VALUES AND DISTRIBUTIONS OF THE FITTED PDFS OF ABSOLUTE ERRORS WHEN USING DIFFERENT THD ESTIMATION METHODS

	Mean value range of AE	Distribution range of AE
Method with calculated THD	0.12% - 0.18%	-0.1% - 0.4%
Method with trained THD	0%	$\pm 0.015\%$

In Fig. 6, when using different estimation approaches, the obtained variation curves of the estimated THD values during the day are combined and compared with an actual THD variation curve for Bus 19. When using the combined ANN training method (ANN1+ANN2), the corresponding MSE of estimated THD is 2.13×10^{-5} , which is 100 times smaller than that of the case considering calculated THD. At the same time, it can be seen from Fig. 6 that in the time domain, the THD variation curve estimated by ANN1+ANN2 is sufficiently accurate and approximately overlapped with the actual THD variation curve. However, the other method tends to result in over estimation of THD values.

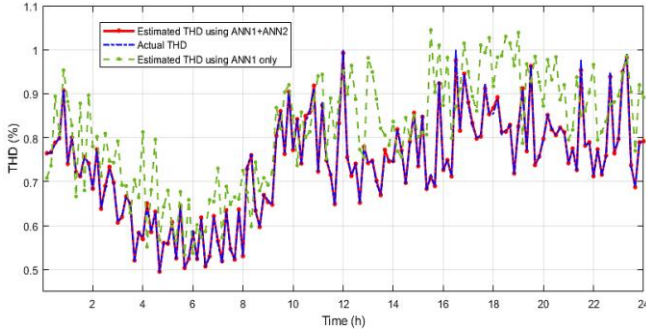


Fig. 6. Comparison of estimated 95th percentile THD during one day at Bus 19 using different THD estimation methods.

Therefore, the method of combining ANN1 and ANN2 optimizes the accuracy of THD estimation at unmonitored buses. The absolute estimation errors have been significantly narrowed down. Thus, this method is recommended as a basic structure of THD prediction in the following studies.

C. Validation of the Combined ANN Model

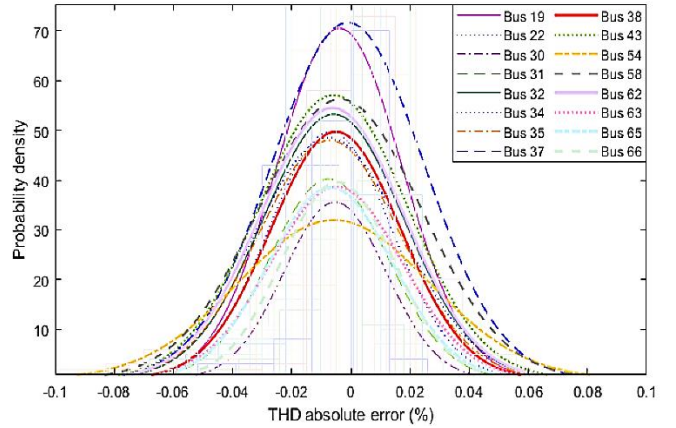
In order to validate the general applicability of the proposed combined ANN structure, harmonic measurements from other weeks (as the target week explained in section III. B) have been obtained by simulating the NETS-NYPS test network. In the beginning, only one-day measurements are considered. The absolute and relative errors of 95th percentile estimated THD are fitted and plotted in Fig. 7 (a) and Fig. 7 (b), respectively.

It can be seen that the mean values of the fitted absolute and relative errors are all approximately concentrated at 0%. According to the distribution span of the fitted absolute error, i.e., $\pm 0.08\%$, and the distribution span of the fitted relative error, i.e., $\pm 10\%$, if the actual THD at the unmonitored bus is 3%, the corresponding estimated value will be within a range from 2.92% to 3.08%, i.e., less than 10% of the actual THD values. Therefore, the combined ANN model performs well and can be used to predict pretty accurately the harmonic distortion at unmonitored buses.

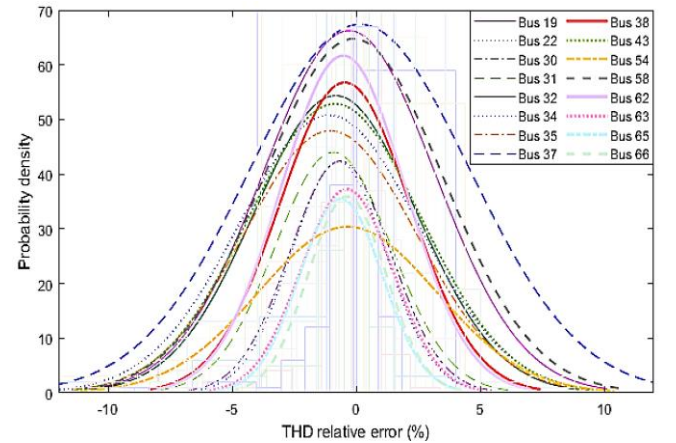
V. CONCLUSIONS

The paper demonstrated the effectiveness and the advantage of the use of sequential ANNs for reliable estimation of harmonic distortion in large transmission networks with uncertain, power electronics interfaced renewable generation. The advantage in terms of accuracy of estimation of THD at unmonitored buses is clearly demonstrated compared to more traditional approach that combines the use of a single ANN for estimation of individual harmonics and conventional formula for calculating THD at unmonitored buses. This preliminary probabilistic study, that will be followed by more rigorous and comprehensive

accuracy assessment in the follow up paper, demonstrates that efficient application of sequential ANNs can contribute to sufficiently accurate assessment of harmonics at unmonitored buses in large uncertain transmission networks and such facilitate identification of potential harmonic issues, deployment of appropriate mitigation solutions, benchmarking and standard compliance without the need for installation of excessive number of power quality monitors.



(a) PDF of absolute error of 95th percentile THD on unmonitored buses.



(b) PDF of relative error of 95th percentile THD on unmonitored buses.

Fig. 7. Fitted PDFs of absolute error and relative error of the 95th percentile THD on unmonitored buses.

ACKNOWLEDGMENT

The authors would like to acknowledge the contributions of Pablo Rodríguez-Pajarón and Araceli Hernández from the Universidad Politécnica de Madrid, for their kindly help with the ANN training tool and generally sharing their knowledge and experience.

This work was supported by the Ministerio de Ciencia, Innovación y Universidades, Spain, under Project RTI2018-097424-B-I00. This paper reflects only the author's views and neither the Agency nor the Commission are responsible for any use that may be made of the information contained therein.

REFERENCES

- [1] Y. Zhao and J. V. Milanović, "Equivalent Modelling of Wind Farms for Probabilistic Harmonic Propagation Studies," *IEEE Transactions on Power Delivery*, vol. 37, no. 1, pp. 603-611, Feb. 2022.

- [2] G. J. Wakileh, *Power Systems Harmonics: Fundamentals, Analysis and Filter Design*. New York, NY, USA; Berlin, Germany: Springer, 2001.
- [3] S. K. Jain and S. Singh, "Harmonics estimation in emerging power system: Key issues and challenges," *Electric power systems research*, vol. 81, no. 9, pp. 1754-1766, 2011.
- [4] A. S. Meliopoulos, F. Zhang, and S. Zelingher, "Power system harmonic state estimation," *IEEE Transactions on Power Delivery*, vol. 9, no. 3, pp. 1701-1709, 1994.
- [5] X. Xiao, Z. Li, Y. Wang, and Y. Zhou, "A Practical Approach to Estimate Harmonic Distortions in Residential Distribution System," *IEEE Transactions on Power Delivery*, vol. 36, Jun. 2021.
- [6] H. Liao, "Power system harmonic state estimation and observability analysis via sparsity maximization," *IEEE Transactions on Power Systems*, vol. 22, no. 1, pp. 15-23, 2007.
- [7] S. O. Haykin, *Neural Networks and Learning Machines, 3rd edition ed.* Pearson Education, 2010.
- [8] H. C. Lin, "Intelligent neural network based dynamic power system harmonic analysis," in *Proc. 2004 International Conf. on Power System Technology*, vol.1, pp. 244-248, 2004.
- [9] Z. Lu, T. Ji, W. Tang, and Q. Wu, "Optimal harmonic estimation using a particle swarm optimizer," *IEEE Transactions on Power Delivery*, vol. 23, no. 2, pp. 1166-1174, 2008.
- [10] S. K. Jain and S. Singh, "Fast harmonic estimation of stationary and time-varying signals using EA-AWNN," *IEEE Transactions on Instrumentation and Measurement*, vol. 62, no. 2, pp. 335-343, 2012.
- [11] S. K. Jain and S. N. Singh, "Low-order dominant harmonic estimation using adaptive wavelet neural network," *IEEE Transactions on Industrial Electronics*, vol. 61, no. 1, pp. 428-435, 2013.
- [12] H. C. Lin, "Intelligent neural network-based fast power system harmonic detection," *IEEE Transactions on Industrial Electronics*, vol. 54, no. 1, pp. 43-52, 2007.
- [13] G. W. Chang, C.-I. Chen, and Y.-F. Teng, "Radial-basis-function-based neural network for harmonic detection," *IEEE Transactions on Industrial Electronics*, vol. 57, no. 6, pp. 2171-2179, 2009.
- [14] G. W. Chang, C.-I. Chen, and Q.-W. Liang, "A two-stage ADALINE for harmonics and interharmonics measurement," *IEEE Transactions on Industrial Electronics*, vol. 56, no. 6, pp. 2220-2228, 2009.
- [15] H. Temurtas and F. Temurtas, "An application of neural networks for harmonic coefficients and relative phase shifts detection," *Expert Systems with Applications*, vol. 38, no. 4, pp. 3446-3450, 2011.
- [16] A. Sarkar, S. R. Choudhury, and S. Sengupta, "A self-synchronized ADALINE network for on-line tracking of power system harmonics," *Measurement*, vol. 44, no. 4, pp. 784-790, 2011.
- [17] S. G. Seifossadat, M. Razzaz, M. Moghaddasian, and M. Monadi, "Harmonic estimation in power systems using adaptive perceptrons based on a genetic algorithm," *WSEAS Transactions On Power Systems*, vol. 11, no. 2, pp. 239-244, 2007.
- [18] J. Mazumdar, R. G. Harley, F. C. Lambert, and G. K. Venayagamoorthy, "Neural network based method for predicting nonlinear load harmonics," *IEEE Transactions on Power Electronics*, vol. 22, no. 3, pp. 1036-1045, 2007.
- [19] J. Mazumdar and R. G. Harley, "Recurrent neural networks trained with backpropagation through time algorithm to estimate nonlinear load harmonic currents," *IEEE Transactions on Industrial Electronics*, vol. 55, no. 9, pp. 3484-3491, 2008.
- [20] S. Abdelrahman, M. Wang, J. V. Milanović and E. Bećirović, "Study of harmonic propagation in transmission networks with high penetration of power electronics devices," in *Proc. 2017 IEEE Manchester PowerTech*, pp. 1-6, 2017.
- [21] J. D. Morales and J. V. Milanović, "Methodology for Optimal Deployment of Corrective Control Measures to Ensure Transient Stability of Uncertain Power Systems," *IEEE Transactions on Power Systems*, vol. 36, no. 3, pp. 1677-1687, May 2021.
- [22] "DIGSILENT Powerfactory user manual version," *DIGSILENT, GmbH*, Gomaringen, Germany, 2018.
- [23] R. D. Zimmerman, C. E. Murillo-Sanchez, R. J. Thomas, "MATPOWER: Steady-state operations, planning, and analysis tools for power systems research and education," *IEEE Trans. Power Syst.*, vol. 26, no. 1, pp. 12-19, Feb. 2011.
- [24] Renewable power plants. [online] Available: https://data.open-power-system-data.org/renewable_power_plants/2020-08-25.
- [25] *IEEE Recommended Practices and Requirements for Harmonic Control in Electrical Power Systems*, IEEE Std. 519, 2014.
- [26] Y. Zhao and J. V. Milanović, "Validation of the Equivalent Model of Wind Farm for Probabilistic Harmonic Propagation Studies," in *Proc. the 26th International Conference and Exhibition on Electricity Distribution*, pp. 845-849, 2021.
- [27] Y. Xu and J. V. Milanović, "Artificial-intelligence-based methodology for load disaggregation at bulk supply point," *IEEE Transactions on Power Systems*, vol. 30, no. 2, pp. 795-803, 2014.
- [28] P. Rodríguez-Pajarón, A. H. Bayo and J. V. Milanović, "Forecasting voltage harmonic distortion in residential distribution networks using smart meter data," *International Journal of Electrical Power & Energy Systems*, vol. 136, pp. 107653, 2022.
- [29] J. Ponočko and J. V. Milanović, "Forecasting demand flexibility of aggregated residential load using smart meter data," *IEEE Transactions on Power Systems*, vol. 33, no. 5, pp. 5446-5455, 2018.
- [30] K. G. Sheela and S. N. Deepa, "Review on methods to fix number of hidden neurons in neural networks," *Mathematical Problems in Engineering*, vol. 2013, pp. 425740, 2013.
- [31] T. Vujicic, T. Matijevic, J. Ljucovic, A. Balota, and Z. Sevarac, "Comparative analysis of methods for determining number of hidden neurons in artificial neural network," in *Proc. Central European Conference on Information and Intelligent Systems*, pp. 219-223, 2016.
- [32] Jin-Yan Li, T. W. S. Chow and Ying-Lin Yu, "The estimation theory and optimization algorithm for the number of hidden units in the higher-order feedforward neural network," in *Proc. ICNN'95 - International Conference on Neural Networks*, vol. 3, pp. 1229-1233, 1995.
- [33] S. Xu and L. Chen, "A novel approach for determining the optimal number of hidden layer neurons for FNN's and its application in data mining," in *Proc. 5th International Conference on Information Technology and Applications*, pp. 683-686, 2008.
- [34] K. Shibata and Y. Ikeda, "Effect of number of hidden neurons on learning in large-scale layered neural networks," in *Proc. 2009 ICCAS-SICE*, pp. 5008-5013, 2009.
- [35] D. Hunter, H. Yu, M. S. Pukish III, J. Kolbusz, and B. M. Wilamowski, "Selection of proper neural network sizes and architectures—A comparative study," *IEEE Transactions on Industrial Informatics*, vol. 8, no. 2, pp. 228-240, 2012.
- [36] Z. Zhang, X. Ma, and Y. Yang, "Bounds on the number of hidden neurons in three-layer binary neural networks," *Neural networks*, vol. 16, no. 7, pp. 995-1002, 2003.
- [37] *Voltage characteristics of electricity supplied by public electricity*, EN Std. 50160, 2010.